Artículo de investigación

Researching of a vacuum pump system based on the numerical computations

ИССЛЕДОВАНИЕ СИСТЕМЫ ВАКУУМНОГО НАСОСА НА ОСНОВЕ ЧИСЛЕННЫХ РАСЧЕТОВ

Recibido: 12 de agosto del 2019 Aceptado: 19 de septiembre del 2019

Written by:
Rishat Salakhov[127]
ORCID ID: 0000-0002-0127-5212
Andrey Ermakov[128]
ORCID ID: 0000-0002-5576-8848
Renat Khismatullin[129]
ORCID ID: 0000-0003-3652-188X

Abstract

This article explores the operation of the GB5601 vacuum pump system created by Engineering GmbH based on the 1D model. The system includes a root pump and a liquid ring vacuum pump. The main objective of the study is to develop and verify a numerical model of a vacuum pump system for analysis in various operating modes. Performance assessment was carried out in the software Simcenter AMESim 1D, where the models are assembled in the libraries Signal, Control, Pneumatics and Thermal.

Keywords: Simcenter AMESim, 1D modeling, vacuum system, Roots booster, liquid-ring vacuum pump.

Аннотация

В этой статье рассматривается работа системы вакуумных насосов GB5601, созданной Engineering GmbH на основе модели 1D. Система включает корневой насос и жидкостный кольцевой вакуумный насос. Основной целью исследования является разработка и проверка численной модели вакуумной насосной системы для анализа в различных режимах работы. Оценка производительности проводилась в программном обеспечении Simcenter AMESim 1D, где модели собраны в библиотеках Signal, Control, Pneumatics и Thermal.

Ключевые слова: Симцентр AMESim, 1D моделирование, вакуумная система, бустер Roots, жидкостно-кольцевой вакуумный насос.

Introduction

Vacuum technology is one of the most widespread technologies in the contemporary industry. The first vacuum pump developed by Otto von Guericke in 1650 made it possible to use rarefied air in almost all areas of life - from household appliances to satellites. Despite widespread use, calculating the behavior of the working medium for gas is rather difficult, especially in an interfaced system with two vacuum pumps. Calculations are performed manually with parameters selected from the technical data tables depending on the differential pressure (PromHimTech, 2003).

This study did not receive any specific grant from funding agencies in the public, commercial or non-profit sectors.

[127] Kazan State Technical University named after A. N. Tupolev – KAI, Kazan, Russia
[128] Kazan State Technical University named after A. N. Tupolev – KAI, Kazan, Russia
[129] Kazan State Technical University named after A. N. Tupolev – KAI, Kazan, Russia

Metodology

The object of simulation is the existing vacuum pump system manufactured by ZM Engineering.

The model simulates only the gas contour (red highlight in Figure 1) except separator and filter.

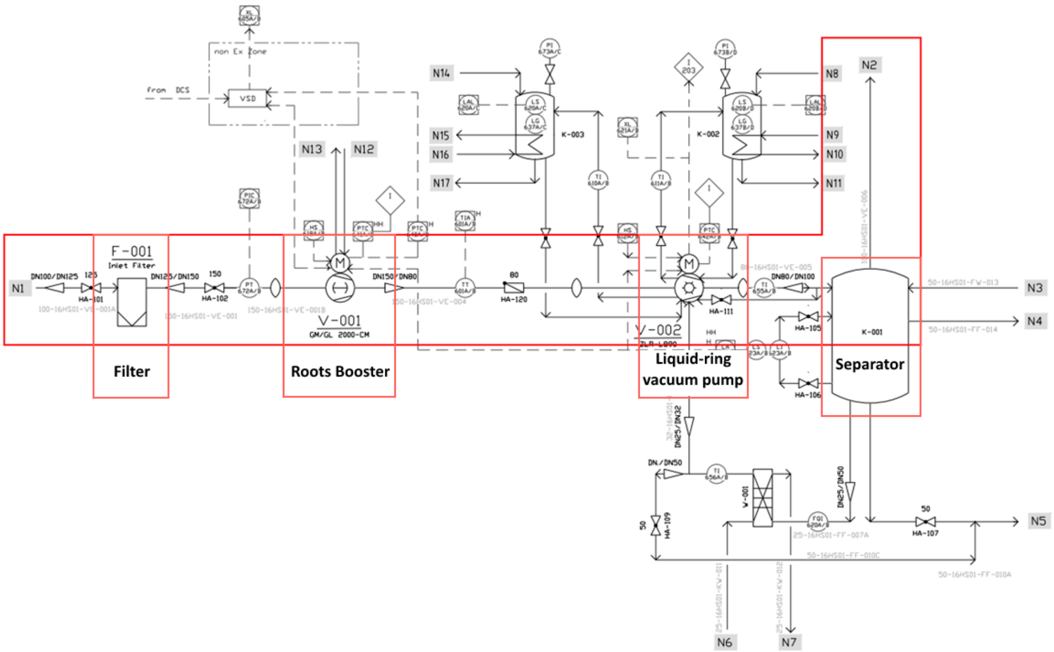

Figure 1. The principal scheme of the GB5601 system: Filter, Roots Booster, Liquid-ring vacuum pump, Separator

The heat transfer between the liquid and the gas inside the liquid ring vacuum pump (LRVP) simulates through two separate models: a gas compressor, and the second PID controller, which reduces the temperature to preset values.

According to the technical requirements of the installation, the following boundary conditions are established:

- Inlet pressure is 10 mbarA;
- Outlet pressure is 1230 mbarA;
- Otlet temperature is 40 °C.

The vacuum pump installation model in Simcenter AMESim

The authors developed a 1D model of the system in Simcenter AMESim software (Figure 2) in accordance with the following works (Rundo 2017; Wang et al., 2017; Mouloud et al., 2011; Guangyu et al., 2016; Pugi et al., 2014; Kopczynski, et al., 2019).

ISSN 2322- 6307

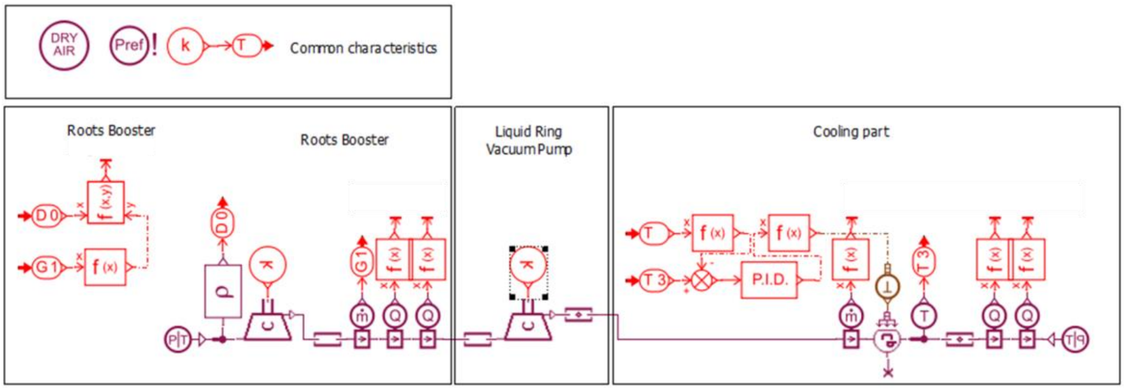

Figure 2. The model of the vacuum pump system GB5601 in Simcenter AMESim: Common characteristics, Roots Booster Qlocal inlet

The model includes the next parts:

1. Submodels characterizing the physical properties of the environment, atmospheric features and the required temperature of the gas at the outlet of the system.
2. The Roots Booster pump.
3. The liquid-ring vacuum pump.
4. Cooling contour.

Description of the environment physical properties.

Submodels characterizing the physical properties of the environment, atmospheric features, and the required gas temperature at the system exit are shown in Figure 3.

Figure 3. The submodels of properties, atmosphere and gas temperature at the outlet

Air is selected as a working fluid with ideal properties. It should be noted that the main property is the density, which varies depending on the temperature value (Figure 4). The corresponding curves are created in accordance with the polynomial equations in the NASA catalog (McBride Bonnie and Zehe Michael, 2002).

ISSN 2322- 6307

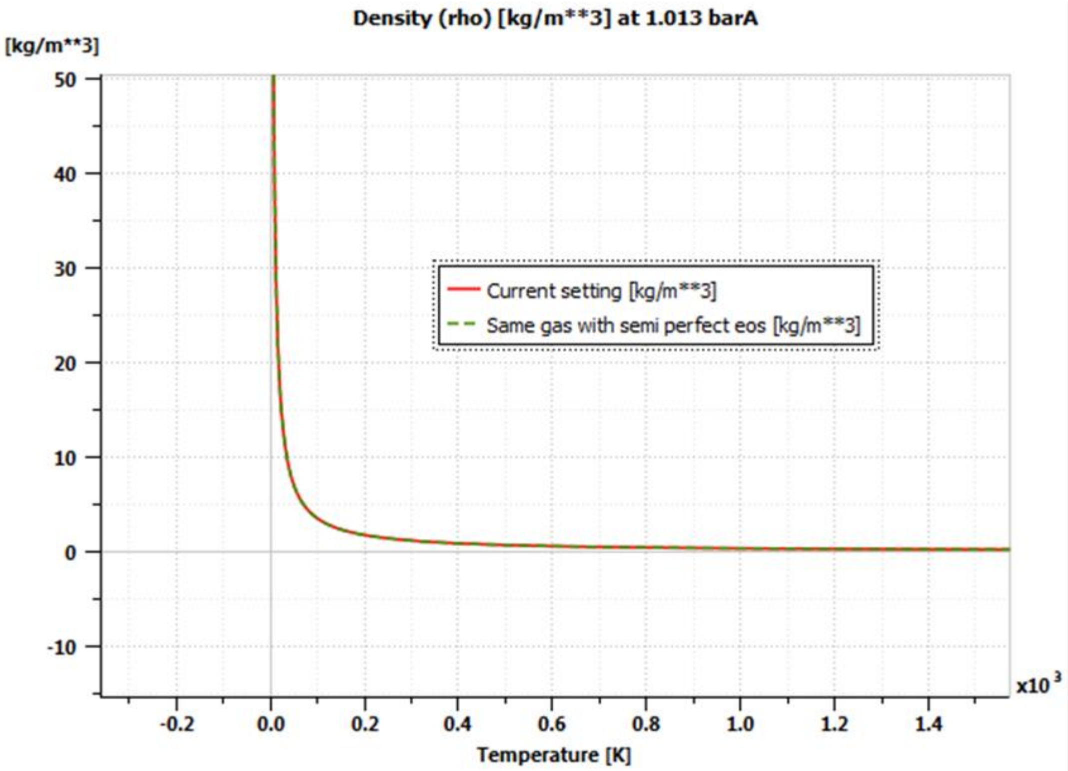

Figure 4. The density gas curve

Atmosphere pressure is 101325 Pa, the outlet gas temperature is 40 °C, density is 1.183624 $\frac{kg}{m^3}$, specific heat is 1004,725480 $\frac{J}{kg \cdot K}$, absolute viscosity is 0,018463, thermal conductivity is 0,026027 $\frac{W}{m \cdot K}$.

Roots Booster pump in the model showed in Figure 5.

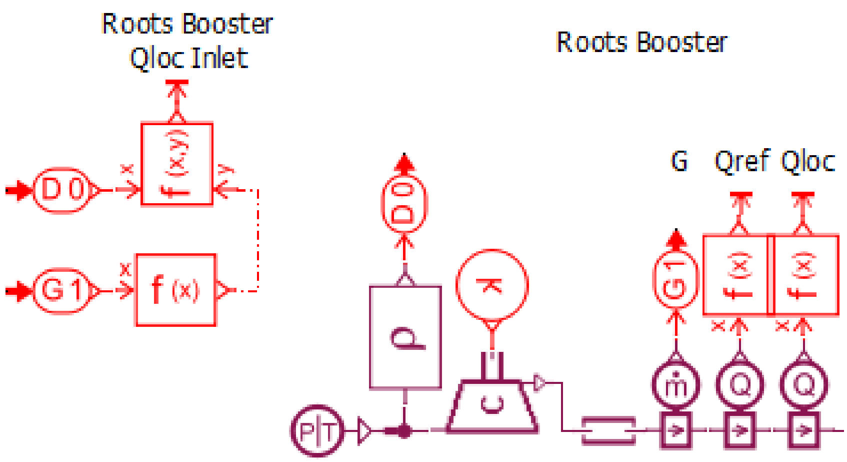

Figure 5. Roots Booster pump in the model

The roots booster pump is modeled on the basis of a standard air compressor operating under vacuum in accordance with the peer-reviewed works (Heng, et al., 2018; Arztmann, 2008; Sadovskiy, et al., 2018). A series of calculations were performed for each frequency of the roots booster pump shaft. This is necessary for interpreting the data received from Aerzen (Figure 6) to the AMESim software format required by Simcenter.

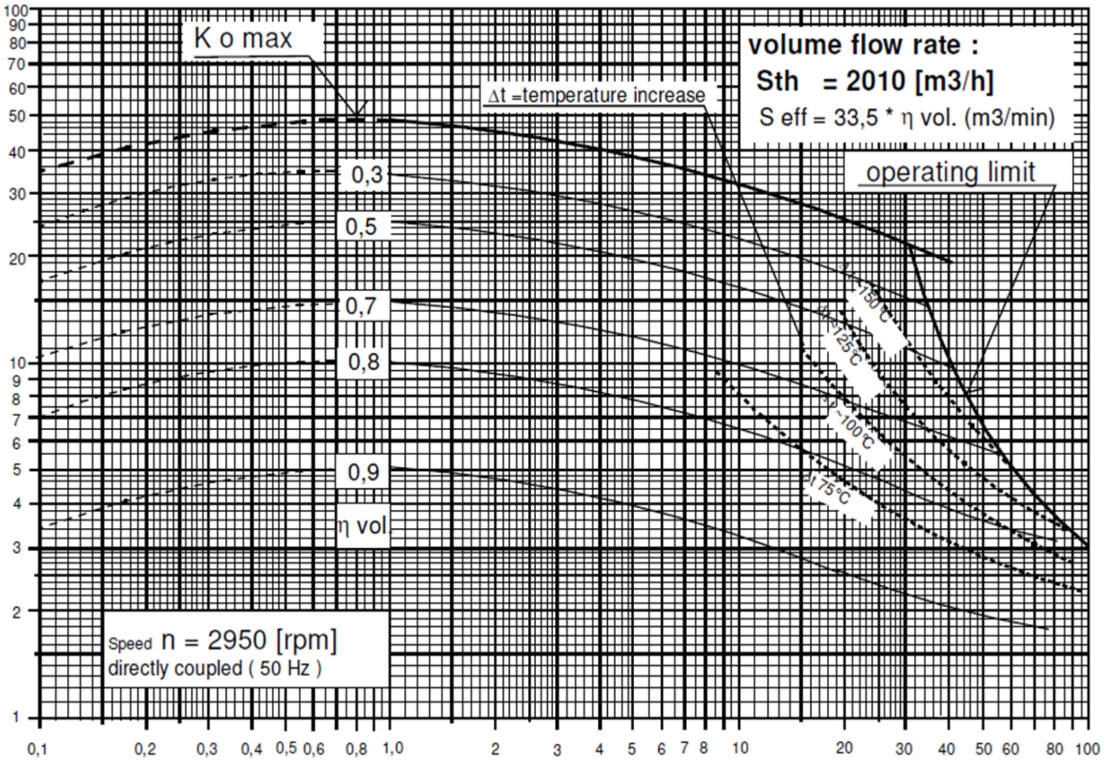

Figure 6. Characteristic curves of the roots booster Pump at 2950 r/min from Aerzen data

The software AMESim requires table data in format Pressure ratio = f (dm ($\frac{kg}{s}$), w ($\frac{r}{min}$)) for compressor submodel. The curves of dependence compression ratio π_k and mass flow rate were compiled for obtaining the table data at each work modes of the engine with different values at the inlet (Figure 7 depicts curves at 1800 $\frac{r}{min}$ roots vacuum pump).

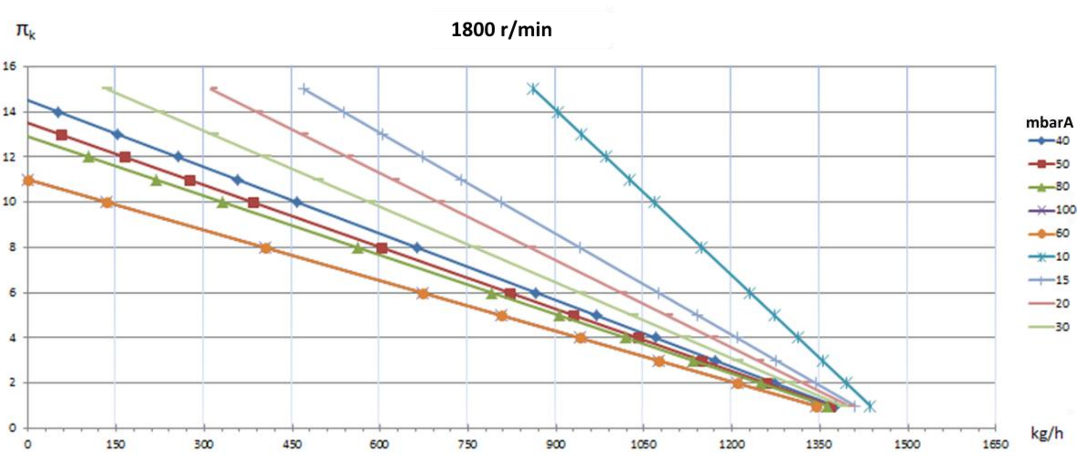

Figure 7. Dependence of compression ratio πk and mass flow rate at 1800 $\frac{r}{min}$ work mode

ISSN 2322- 6307

These results presented in the Simcenter AMESim software and the following performance data are shown in Figure 8. At the current stage, we manually installed data files for each pressure value at the pump inlet for adequate model operation.

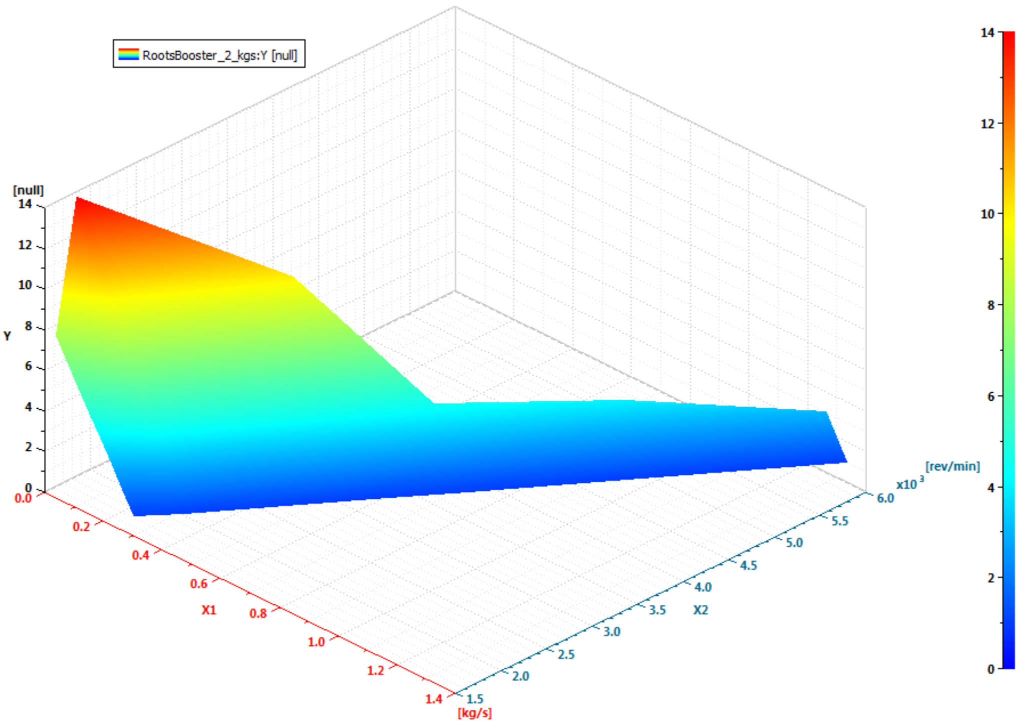

Figure 8. The pump characteristics in Simcenter AMESim software

To determine the relationship between volumetric efficiency, inlet pressure, and compression ratio efficiency, a series of calculations were performed in a separate root amplifier model (Figure 9). At the next step, for each mode, an approximation was carried out and linear trend equations were created (Table 1), where x - mass flow ($\frac{kg}{s}$), y - compression ratio π_k.

Table 1. The equations of linear trend of the roots booster pump

r/min	Trend equation
1500	$y = -23{,}428 \cdot x + 32{,}603$
1800	$y = -21{,}631 \cdot x + 24{,}516$
3000	$y = -22{,}094 \cdot x + 19{,}214$
3600	$y = -20{,}395 \cdot x + 15{,}596$
4800	$y = -25{,}197 \cdot x + 11{,}352$
6000	$y = -21{,}186 \cdot x + 7{,}9958$

ISSN 2322- 6307

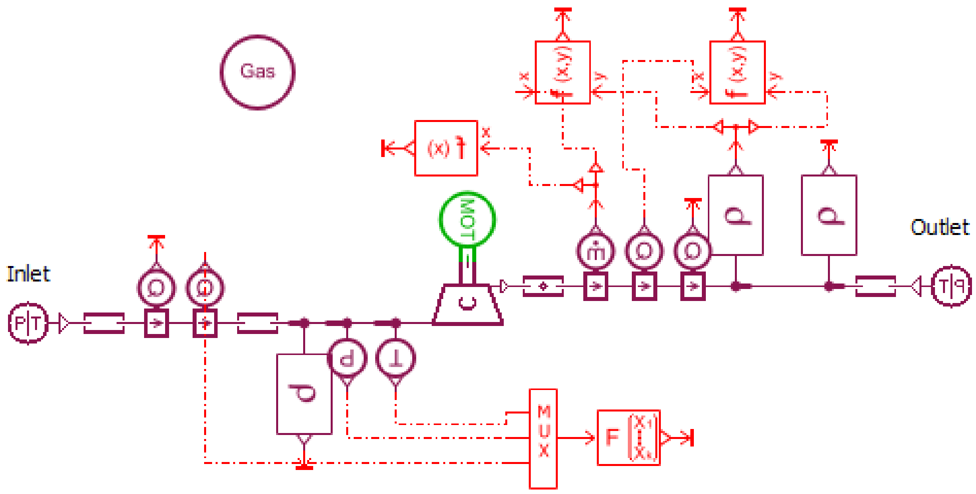

Fig 9. The single roots booster pump model

The calculated curves transported to the Simcenter AMESim software became to look according to Figure 10.

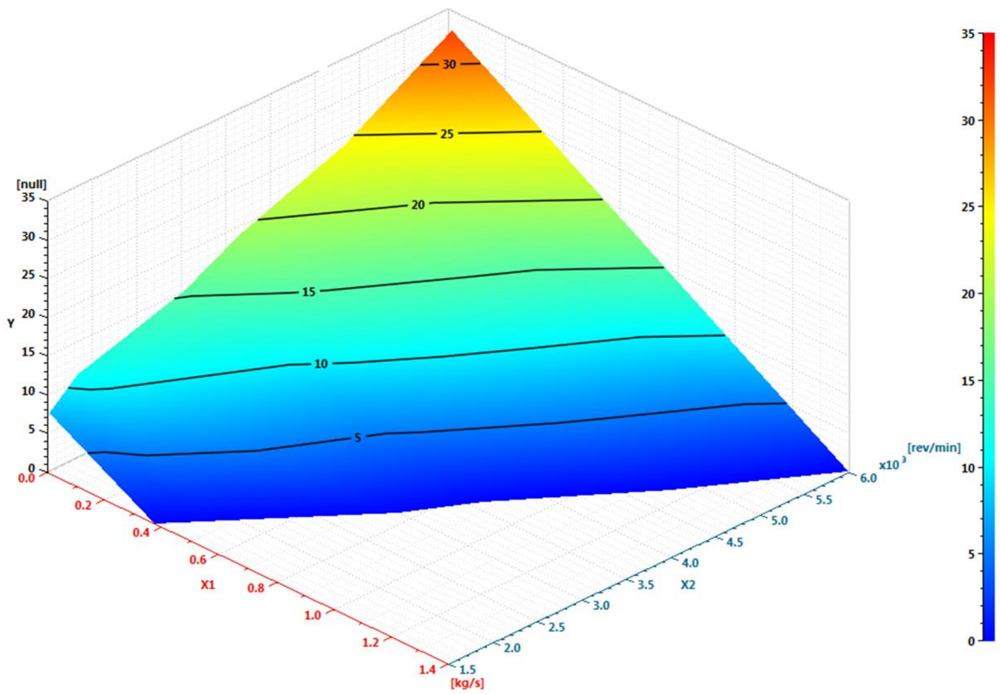

Figure 10. The final roots booster pump characteristic in Simcenter AMESim software

The convergence of the results corresponded to Aerzen technical data when modeling the model in various modes after introducing the calculated characteristics of the roots booster pump into the Simcenter AMESim software. Thus, the pump model can be used in other similar models.

Liquid-ring vacuum pump showed in Figure 11.

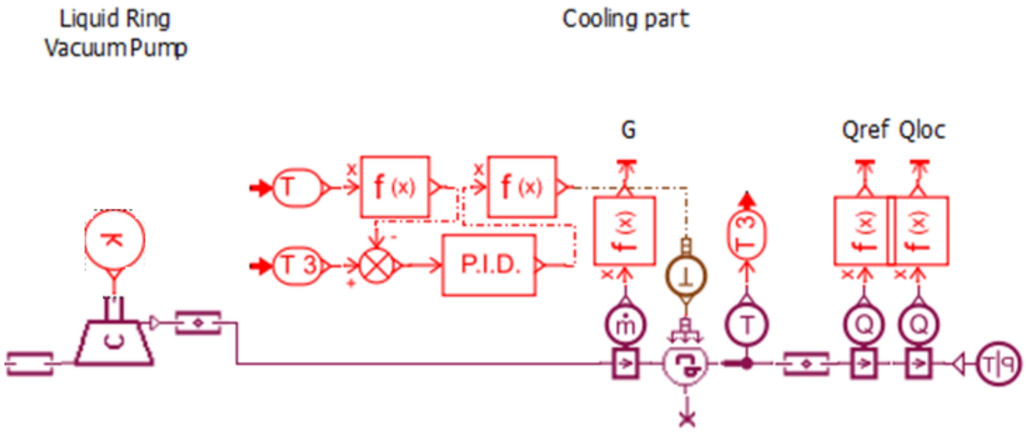

Figure 11. Liquid-ring vacuum pump part in the model

The LRVP model based on the explored works (Prananto et al. 2017; Bannwarth, 2005; Olšiak et al., 2018; Levchenko et al., 2011) and divided into 2 parts:

1. Gas compressor part.
2. Heat exchange part
3. Gas compressor

To simulate gas compression in LRVP, we used a submodel of a simple gas compressor. The inlet temperature and pressure values are transferred from the root output of the roots booster pump. The outlet pressure is 1230 mbar (indicated in the user requirements).

The characteristic of the liquid-ring vacuum pump described in Figure 12.

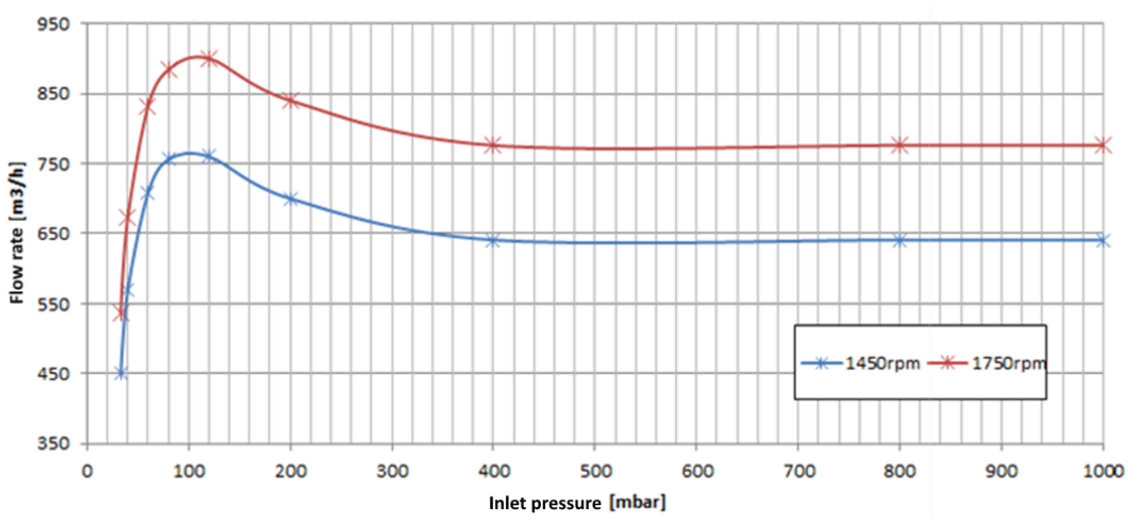

Figure 12. The received characteristic curves of LRVP

Simcenter AMESim software requires a minimum of 3 curves for adequate calculation, so the characteristic curve was interpolated at 1600 rpm of the pump. In addition to interpolation, all the curves were expanded to almost zero flow. The volumetric flow rate values are transferred to the mass flow rate unit. Y axis size has been changed to compression ratio $\pi_k = \frac{p_{in}}{p_{out}}$, where p_{in} noted accordingly to the x-axis values in the Figure 12, mbarA; p_{out} = 1013 mbarA, due to the design of curves calculated under standard conditions. It should be noted that AMESim does not perceive the opposite change in the angle of the curve after 120 mbar, therefore, the gas flow rate does not decrease depending on the increase in pressure, but remains constant. The last assumption is accepted, because in actual operation the LRVP does not work in high-pressure modes. The final calculated curves of the liquid ring vacuum pump shown in Figure 13, and their interpretation in the Simcenter AMESim software in Figure 14.

ISSN 2322- 6307

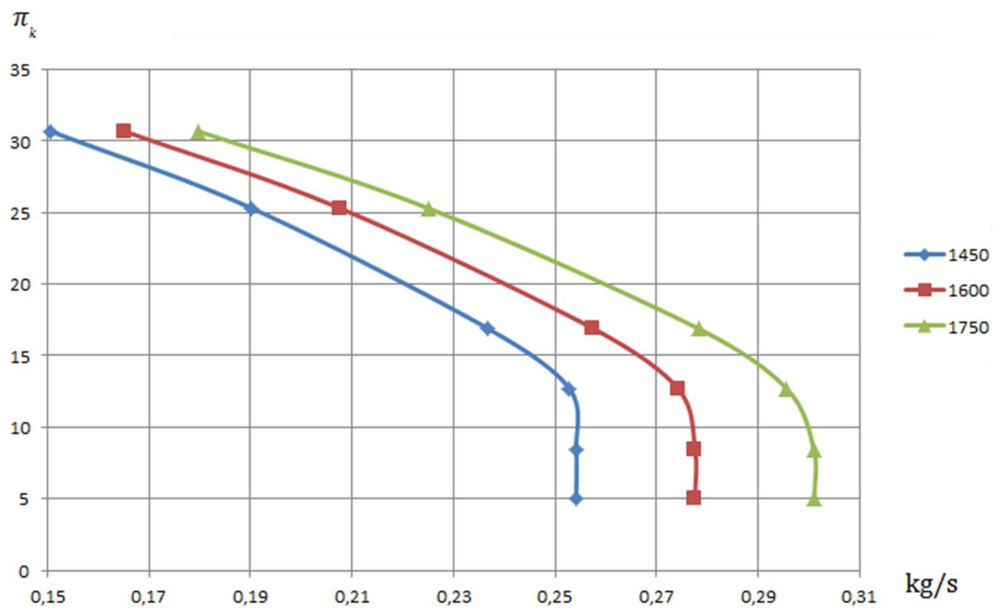

Figure 13. The recalculated characteristic curves of LRVP

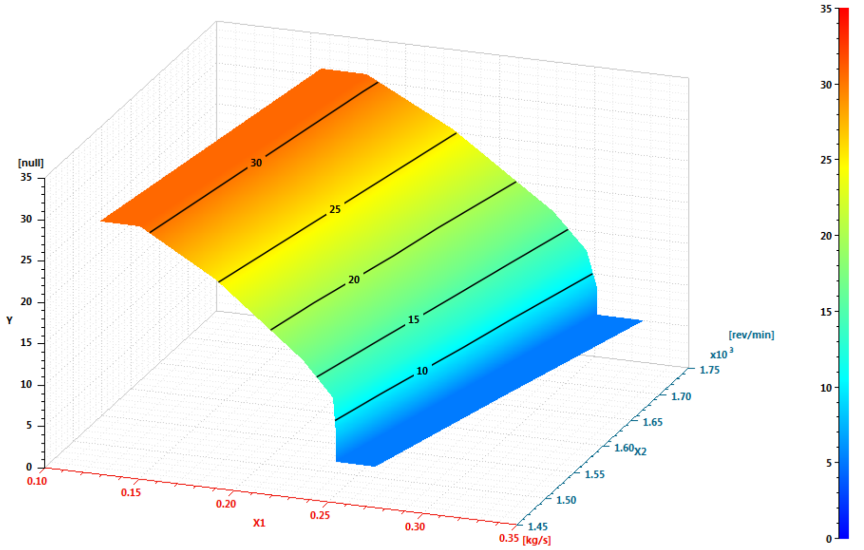

Figure 14. The recalculated characteristic curves of LRVP in Simcenter AMESim software

If the characteristic curves are entered into Simcenter AMESim and the constant outlet pressure is 1230 mbar, the simulation results will display values in accordance with the technical data for various operating modes and inlet pressures.

One of the most important features of the model, which includes two vacuum pumps, is the need to bring together the performance map of both vacuum pumps in each operating mode. At the current stage of model development, there are no common ground between the LRVP and the root amplifier, therefore, the model is disconnected due to a failure of the convergence stream of the stream. Theoretically, the model should work according to the following algorithm: the pressure at the outlet of the roots booster pump increases, while the flow rate in the liquid ring vacuum pump remains at its original value. Implementation of the aforementioned logic requires modification of the current characteristic curves in the range above 120 mbar to a higher flow rate (Figure 15). It is worth noting that this assumption is reasonable, since the real installation is not used in similar operating modes.

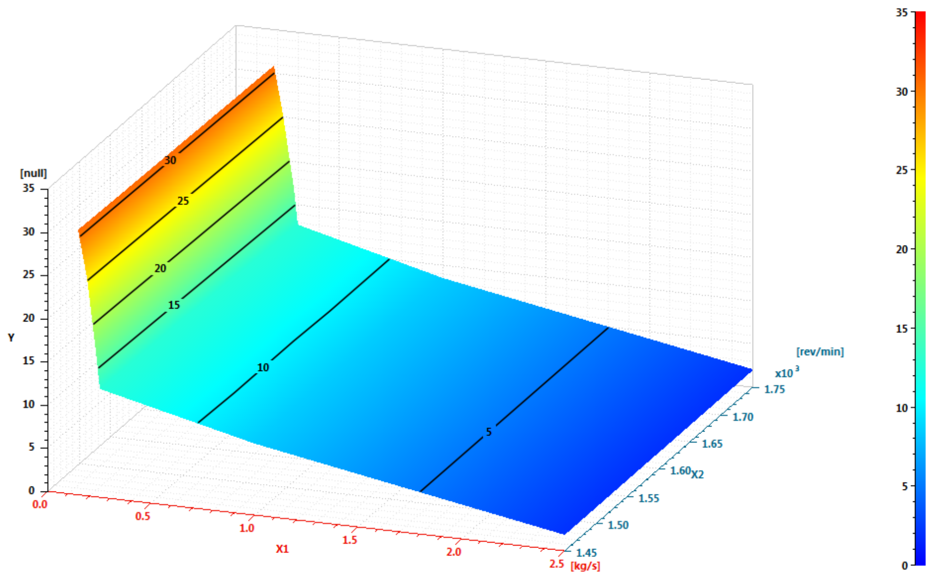

Figure 15. LRVP characteristic with the flow rate assumption

Simulation of heat transfer between a gas and a liquid phase in a liquid-ring vacuum pump, modeled on the basis of articles (Salakhov et al., 2017; Misbakhov et al. 2015).

Temperature stabilization after LRVP is carried out using a PID controller installed at the output of the model due to the lack of calculated data and calculation methods. The temperature in the PID controller drops to the set value (default value is 40°C).

Work principle and verification

Figure 16 depicts the stages of the model work.

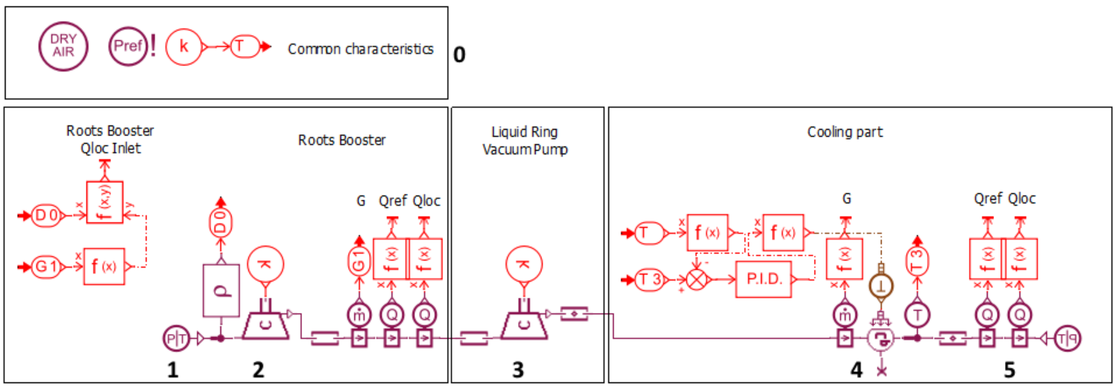

Figure 16. Working stages of the model

0. At each stage of the calculation, the model requests submodels of the working fluid and the state of the atmosphere.
1. Gas enters the model at the inlet with predetermined temperature and pressure parameters (1 ° C and 10 mbar, respectively).
2. The gas is compressed and heated in the roots booster pump and passes through the mass and volume flow detectors to the next stage.
3. The compressor part of the vacuum-liquid vacuum pump uses gas selected from the roots booster pump outlet and increases its temperature and pressure.

ISSN 2322- 6307

4. Hot and compressed gas enters a volumetric container with a heat exchanger, in which the temperature of the working fluid decreases to the temperature noted in the submodels from the first point (the default value is 40°C).

5. Compressed gas is discharged out of the system.

Results and discussion

Verification of the model was carried out in accordance with the photograph of Nizhnekamsk production at nominal operation mode (Figure 17) and on the basis of technical requirements at the inlet and outlet (Figure 18).

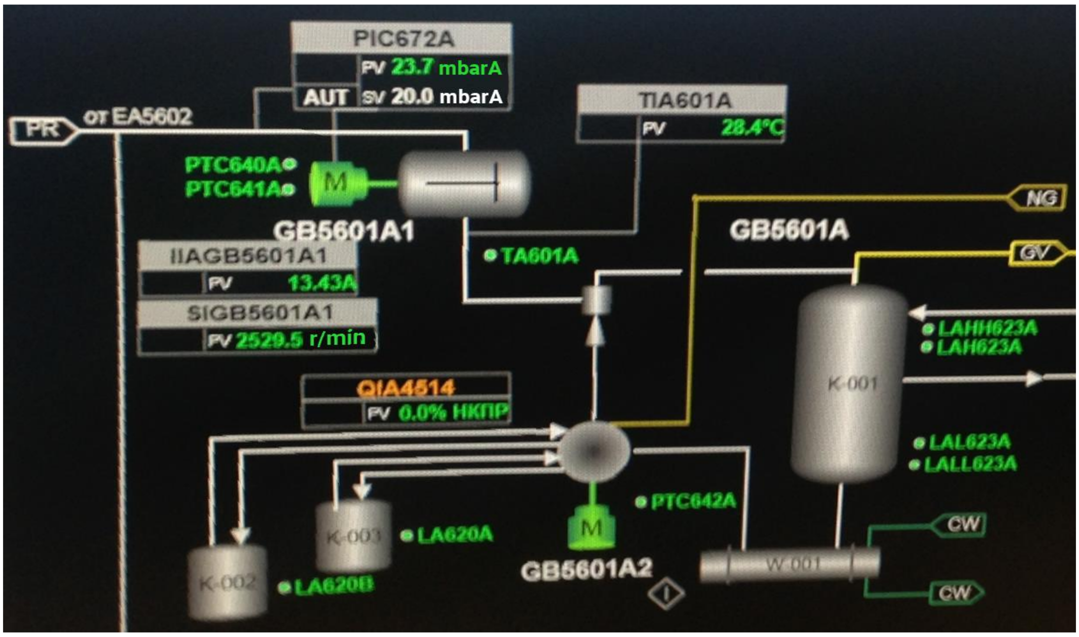

Figure 17. Nominal work mode of the installation GB5601

Figure 17 describes the following useful information:

- The pressure at the inlet of the roots booster pump is 23,7 mbarA.
- The frequency of the roots booster pump is 2529,5 r/min.
- The temperature of the gas at the inlet is 28,4 °C.

RATED FLOW (DRY) Ном. расход (по сух. газу)			(Nm³/h)
INLET VOL. FLOW Объем расход входн.		1175	(m³/h)
TEMP. SUCTION Темп. Всаса		1.0	(°C)
MAX. Макс.	MIN. Мин.		(°C)
TEMP. DISCHARGE Темп. Нагнетания			(°C)
PRESS. DISCHARGE. Давл. Нагнетание		123	(kPaA) (КПа абс.)
SUCTION. Всас		1.066	(kPaA) (КПа абс.)

Figure 18. The actual part of the technical requirements

The technical requirements state the need for pumping out 1175 m3/h at nominal operation at a pressure of at least 1230 mbar.

Values of volumetric flow and pressure are detected in the indicated areas in Figure 19.

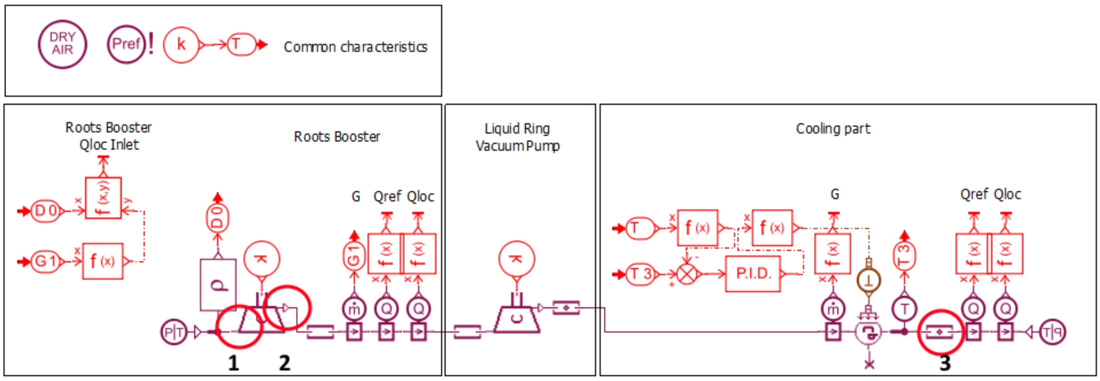

Figure 19. Positions of pressure and flow rate values detecting:
1 – Inlet the system; 2 – roots booster outlet; 3 – outlet the system

The data obtained as a result of modeling at 2529.5 rpm of the roots booster frequency and 1450 rpm of the LRVP frequency are presented in Table 2.

Table 2. Simulation results

	GB5601A	Simcenter AMESim
Inlet pressure, mbarA	23,7	23,70
Standrad volumetric flow rate, nm3/hr	1175	1253,87
Inlet temperature, °C	28,4	28,40
Outlet roots booster pressure, mbarA	40	108,81
Outlet roots booster temperature, °C	104,15	138,09
Outlet pressure, mbarA	1230	1230,97
Outlet temperature, °C	40	41,51
Mass flow rate, kg/hr	1484	1509,43

Based on the results, it can be argued that all the necessary conditions for the specification are met. The relative error is in the acceptable range, therefore, the model is verified.

In this work, the vacuum system model was developed in the Simcenter AMESim software, the pump performance diagrams were recalculated and transferred to the required format in the vacuum model of the roots booster and liquid ring pump. The main problem was identified in the calculations at different operating modes. This is a special pressure curve in the LRVP that has a constant flow rate while decreasing the compression ratio compared to the roots booster pump, which has a standard pump pressure curve. Consumption increases with decreasing compression ratio on the standard curve. The current circumstance can probably be solved by changing the LRVP characteristic curve at a low compression ratio. The latest change allows the model in Simcenter AMESim software to solve the problem of stream convergence.

Conclusion

The GB5601 vacuum pump installation model created by ZM Engineering GmbH was developed in the present work by the Simcenter AMESim software. In addition, the characteristic curves for the vacuum roots booster pump and the liquid ring pump were recalculated and transferred to the corresponding submodels. The numerical model is tested on the basis of a real vacuum setup. Finally, the simulation results for various operating modes of the vacuum pump system are analyzed.

The obtained data on the interpretation of the pressure characteristics of vacuum pumps from technical data sheets in the required Simcenter AMESim format can be used in the calculations of other vacuum plants. This information can help to avoid significant waste of modelling time.

References

1. PromHimTech. (2003). Liquids Ring Vacuum Pumps & Compressors, Technical Details & Fields of Application (7th ed.). Leinfelden-Echterdingen: Sterling fluid systems group.
2. Rundo, M. (2017). Models for Flow Rate Simulation in Gear Pumps: A Review. Energies, 9, 1–32.
3. Wang, Y., Gao, Q., Zhang, T. (2017). Advances in integrated vehicle thermal management and numerical simulation. Energies, 10, 1-30.
4. Mouloud, G., Slimane, A., Ahmed, H. (2011). Flow Measurement and Control in Gas Pipeline System using Intelligent Sonic Nozzle Sensor. Studies in Informatics and Control, 20, 85–96.
5. Guangyu, D., Robert, E., Morgan, R. (2016). Thermodynamic analysis and system design of a novel split cycle engine concept. Energies 102, 576–585.
6. Pugi, L. Conti, R., Rindi, A., Rossin, S. (2014). A thermo-hydraulic tool for automatic virtual HazOp evaluation. Metrology and Measurement Systems, 21, 631 – 648.
7. Kopczynski, A., Malecha, Z., Polinski, J. (2019). Test stand for determination of the heat flux to the cold elements of cryogenic systems in case of the vacuum vessel failure. IOP Conference Series: Materials Science and Engineering, 502, 1–5.
8. McBride Bonnie, J., Zehe Michael, J. (2002). NASA Glenn Coefficients for Calculating Thermodynamic Properties of Individual Species.
9. Heng, Z., Sin, S., Tai, L., Kaijun, D. (2018). Coupling Heat Pump and Vacuum Drying Technology for Urban Sludge Processing. Energy Procedia, 158, 1804-1810.
10. Arztmann, R. (2008). Experience with dry running vacuum pumps in helium service. AIP Conference Proceedings, 53, 316–322.
11. Sadovskiy, N., Strizhak, L., Simonov, A., Sokolov, M. (2018). Some problem of centrifugal compressors upgrading. MATEC Web of Conferences, 245, 512 – 522.
12. Prananto, L., Mu'Min, G., Soelaiman, T., Aziz, M. (2017). Dry steam cycle optimization for the utilization of excess steam at Kamojang geothermal power plant. AIP Conference Proceedings, 1984, 120-134.
13. Bannwarth, H. (2005). Liquid Ring Vacuum Pumps, Compressors and Systems: Conventional and Hermetic Design. Wiley, 246–247.
14. Olšiak, R., Fuszko, Z., Csuka, Z. (2018). Reduction of the suction pressure of a liquid ring vacuum pump with a supersonic gas ejector. MATEC Web of Conference.
15. Levchenko, D., Meleychuk, S., Arseniev, V. (2011). Regime characteristics of vacuum unit with a vortex ejector stage with different geometry of its flow path. Proceedings of the International Scientific and Engineering Conference on Hermetic Sealing, 39, 28-34.
16. Salakhov, R., Khismatullin, R., Gureev, V. (2017). Development of a functional model for the cooling system of a inline six-cylinder diesel engine with modeling the operation of the air conditioning system in the lms amesim software package. International Journal of Mechanical Engineering and Technology, 3(8), 467-475.
17. Misbakhov, R., Gureev, V., Moskalenko, N., Ermakov, A., Bagautdinov, I. (2015). Numerical studies into hydrodynamics and heat exchange in heat exchangers using helical square and oval tubes. Biosciences Biotechnology Research Asia, 12, 719–724.